Supporting Information: Supporting Information: Patchy particle insights into self-assembly of transparent, graded index squid lenses

Irem Altan,[*,†] Viola Bauernfeind,[†,‡] and Alison M. Sweeney[*,†,¶]

†*Department of Physics, Yale University, New Haven, USA*

‡*Faculty of Science and Medicine, Fribourg, Switzerland*

¶*Department of Ecology and Evolutionary Biology, Yale University, New Haven, USA*

E-mail: irem.altan@yale.edu; alison.sweeney@yale.edu

Monte Carlo Simulations

As mentioned in the main text, our simulation procedure is not likely to result in equilibrium gels. Similarly, we know that the structures in the squid are highly regular because they are highly transparent, and therefore are likely close to an energetic minimum, but we do not know how close they may be to a state of physical equilibrium. Therefore, our goal is to anneal the systems to low enough temperatures to form configurations with structures similar enough to both the transparent squid structures and to final equilibrium gel to merit structural analysis. We assess the quality of our sampling in this regard by calculating autocorrelation functions for displacement of particles, $C_p(t)$, as well as the energy per particle, $C_e(t)$. Positional autocorrelation is calculated as

$$C(t) = \frac{1}{N}\sum_{i=1}^{N}\Big[1 - \Theta(\sigma - |\mathbf{r}_i(t) - \mathbf{r}_i(0)|)\Big], \tag{1}$$

where the sum runs over all particles, $\mathbf{r}_i$ gives the position vector of the i$^{\text{th}}$ particle, Θ is the Heaviside function, and σ is the particle diameter. A particle is thus considered to have decorrelated from its original position if it has moved by at least one particle diameter, and the positional autocorrelation function quantifies the fraction of particles that have not decorrelated from their position at $t = 0$ at a given time t. The autocorrelation for energy is calculated as

$$C_e(t) = \frac{1}{\mathcal{N}}\sum_{t'=t_s}^{N_{\text{frames}}-t}\sum_{t''=0}^{t}(E(t'+t'') - \langle E\rangle)(E(t') - \langle E\rangle), \tag{2}$$

where $E(t)$ is the energy at time t, $\langle E\rangle$ is the ensemble average of E, t_s is the time from the averaging begins (in our case $t_s = 2N_{\text{frames}}/3$), and $\mathcal{N}$ is a normalization factor chosen such that $C_e(0) = 1$.

Fig. S1a shows $C_p(t)$ and Fig S1b shows $C_e(t)$ for various temperatures. A sum of two exponentials were fit to the autocorrelation data to extract correlation times, τ_α, and the larger τ_α value is reported in the legends. For $\theta = 180°$, the positions of particles are well sampled down to $\beta = 12$, while for smaller θ, this is the case for $\beta = 20$ or so. It is likely, for $\theta < 180°$, that the patch geometry allows the particles to wiggle around without breaking bonds, at low temperatures, allowing for sufficient displacement, especially for trimers and tetramers. The decorrelation of energy per particle is thus more informative. Fig S1b suggests that for all θ, the sampling down to $\beta \sim 10 - 15$ is adequate. Note that for some of these systems, $C_e(t)$ for higher β are not reported, as the energy per particle does not change sufficiently to allow for the calculation of $C_e(t)$. Also note that increasing M increases the autocorrelation time, as seen in Fig. S2. This is expected, as increasing M increases the

average stickiness of the patches.

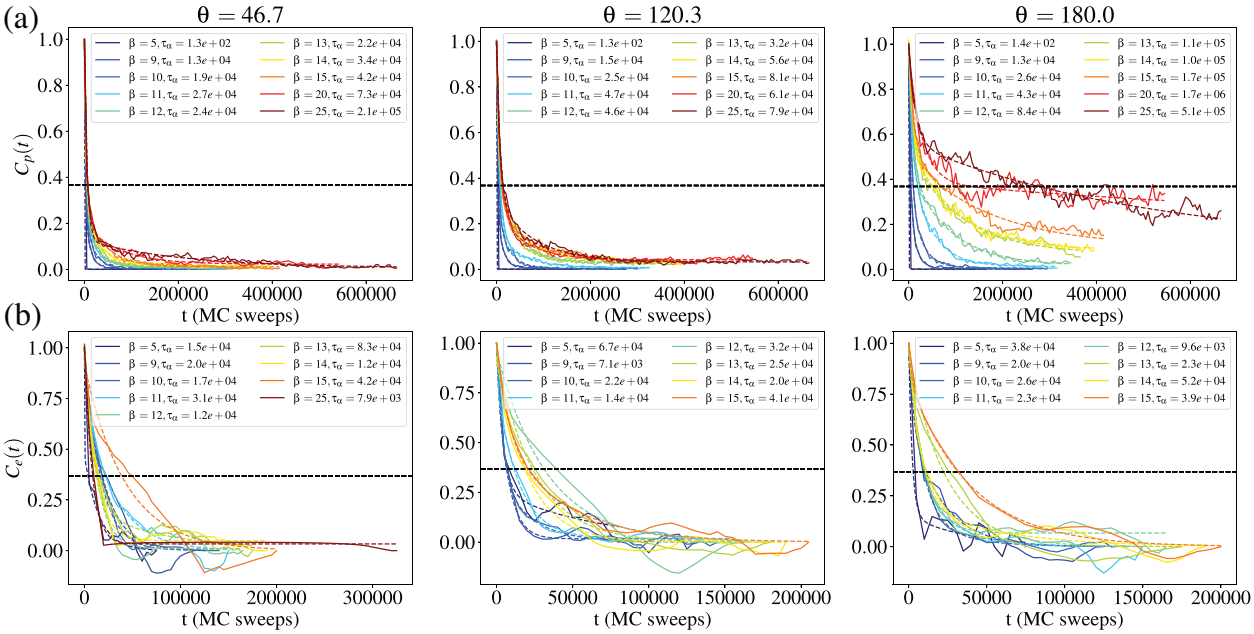

Figure S1: **(a)** Autocorrelation functions for particle positions, $C_p(t)$, for various β and θ values. **(b)** Autocorrelation functions for energy per particle, $C_e(t)$. The legends show τ_α values extracted from exponential fits to the data. The black dashed lines show $\exp(-1)$, the intersection of which with the autocorrelation functions roughly corresponds to $t \sim \tau_\alpha$.

Similarly, Fig S3 shows $C_p(t)$ and $C_e(t)$ for simulations with different σ_ε. σ_ε does not seem to have an effect on the relaxation timescales, but as σ_ε increases, the fraction of particles that do not decorrelate from their positions during the simulation (as indicated by the tail value of $C_p(t)$) decreases. This is consistent with there being a few, less attractive patches in the ε distribution. While the relaxation timescales suggest that all β are sufficiently sampled by our simulations, the fraction of stuck particles is non-negligible at higher β. We thus treat the results of these simulations as structures representative of the gel.

Radial Distribution Functions and Structure Factors

As ϕ increases, the peak heights in $g(r)$, as well as the trough depths, decrease (Fig. S4). At a first glance this might be counterintuitive, as the average coordination number at a given distance r is expected to grow with ϕ. The running coordination number, $N(r)$, gives the

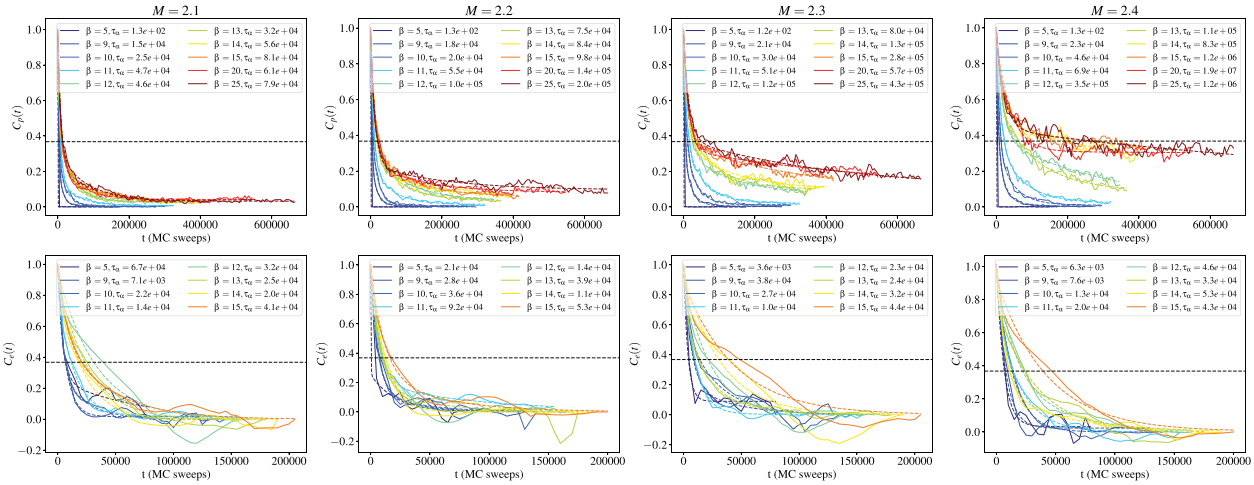

Figure S2: **(a)** Autocorrelation functions for particle positions, $C_p(t)$, for various β and M values, for $\theta = 120.3°$. **(b)** Autocorrelation functions for energy per particle, $C_e(t)$ for the same systems. The legends show τ_α values extracted from exponential fits to the data. The black dashed lines show $\exp(-1)$, the intersection of which with the autocorrelation functions roughly corresponds to $t \sim \tau_\alpha$.

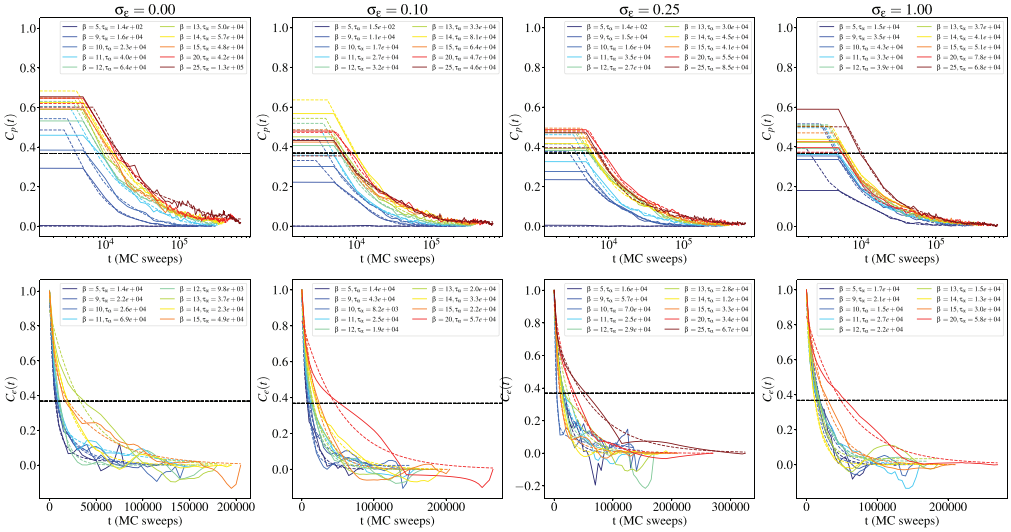

Figure S3: **(a)** Autocorrelation functions for particle positions, $C_p(t)$, for $\theta = 120.3°$, $M = 2.1$, and $N = 1024$ for different σ_ε values. **(b)** Autocorrelation functions for energy per particle, $C_e(t)$. The legends show τ_α values extracted from exponential fits to the data. The black dashed lines show $\exp(-1)$, the intersection of which with the autocorrelation functions roughly corresponds to $t \sim \tau_\alpha$.

average number of particles within a distance r from a particle in the system, and is defined as

$$N(r) = 4\pi\rho \int_0^r g(r')r'^2 dr'. \tag{3}$$

The coordination numbers starting from the nearest neighbor peak in $g(r)$ are higher for denser systems, as expected (Fig. S5(a)). While this holds for all M, the difference between the $N(r)$ curves is a bit diminished for larger M (Fig. S5(b)) Since we are at very low temperatures, the number of nearest neighbors of a given particle is dictated by the average valence of the system. For sufficiently high densities, this number is also contributed to by clusters that are close to each other. Or, if the connectivity of clusters allows it, the proximity of chains within the cluster can also increase the first coordination number. The average valence and the cluster geometry may thus limit the coordination number increase with increasing ϕ, in comparison with a fluid.

In addition, the suppression in height (and depth) of peaks (troughs) in $g(r)$ for high ϕ suggests that the analyzed systems have smaller density fluctuations. This observation is in line with the fact that the density fluctuations should decrease as one moves away from the binodal.

Further, as noted in the main text, the geometric predictions for the location of the next-nearest neighbor peak breaks down as M is increased (Fig. S7).

Finally, Fig. S8 shows the structure factors for $M = 2.1$ for all ϕ and four different θ values. As mentioned in the main text, an additional peak or shoulder emerges at around $q = 0.03\mathring{A}^{-1}$ for smaller θ, and becomes more pronounced as ϕ increases.

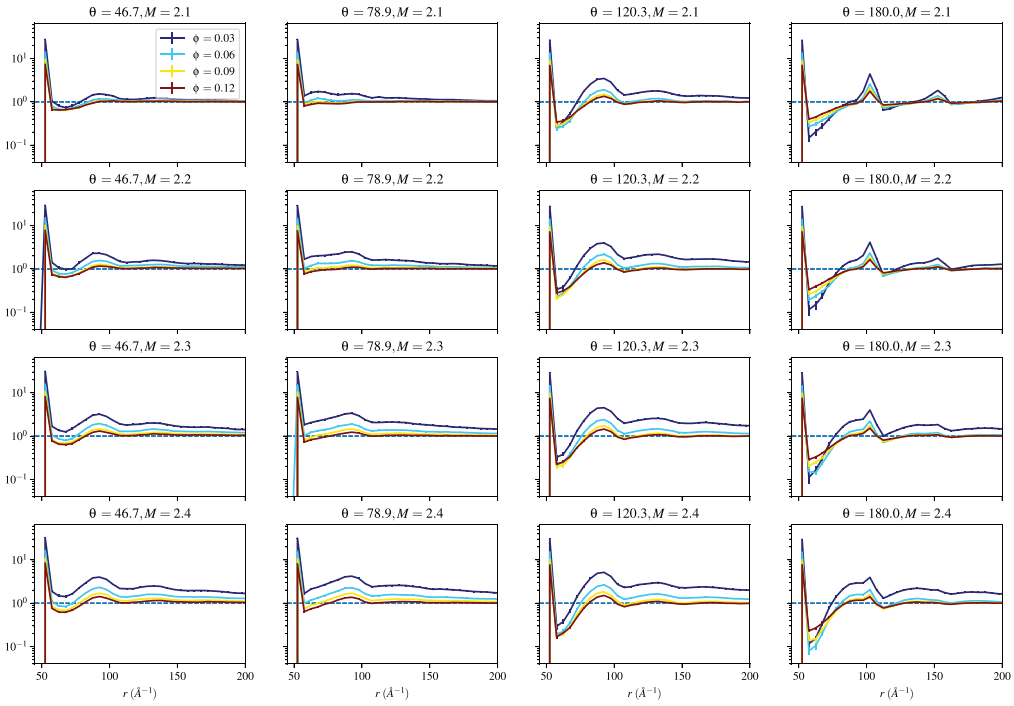

Figure S4: Radial distribution functions for different θ, M values, comparing the effect of ϕ.

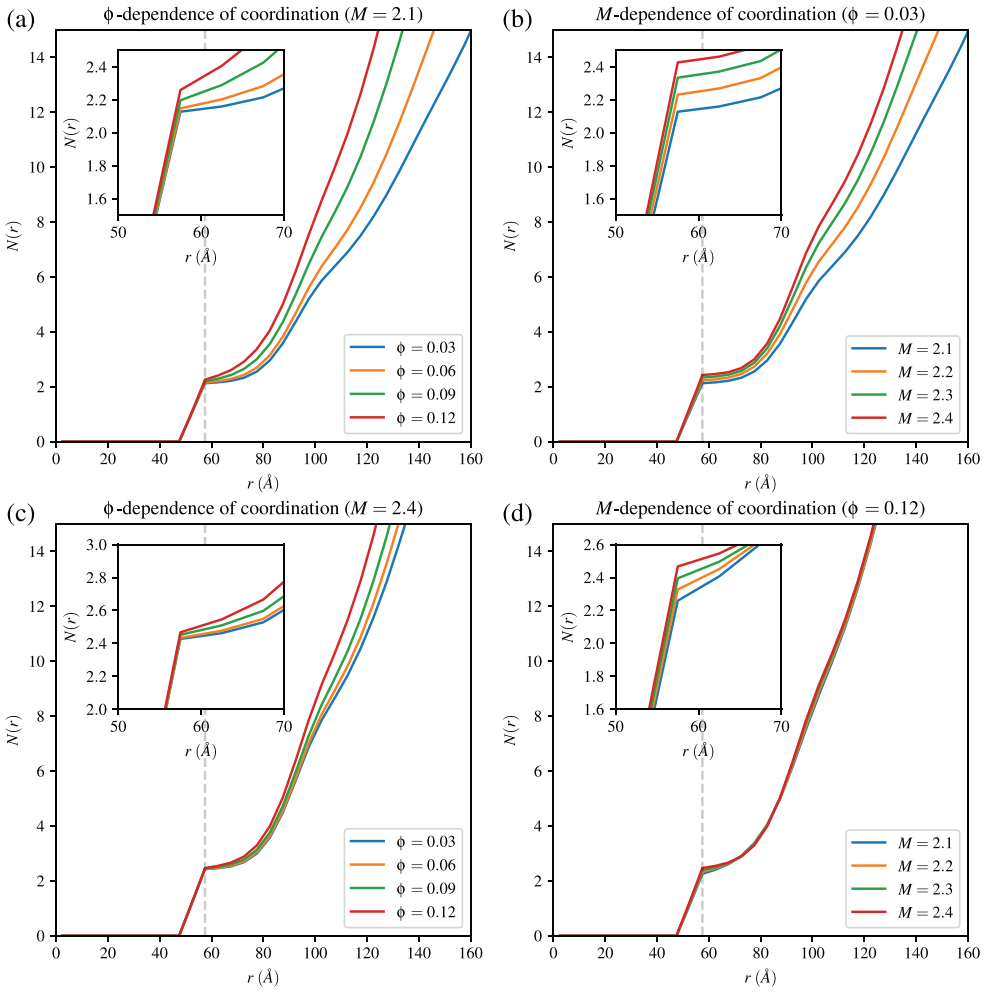

Figure S5: Coordination numbers as calculated by integrating $g(r)$. **(a)** and **(c)** show the effect of ϕ on coordination numbers, for $M = 2.1$ and $M = 2.4$, respectively. **(b)** and **(d)** show the effect of M on coordination numbers, for $\phi = 0.03$ and $\phi = 0.12$, respectively.

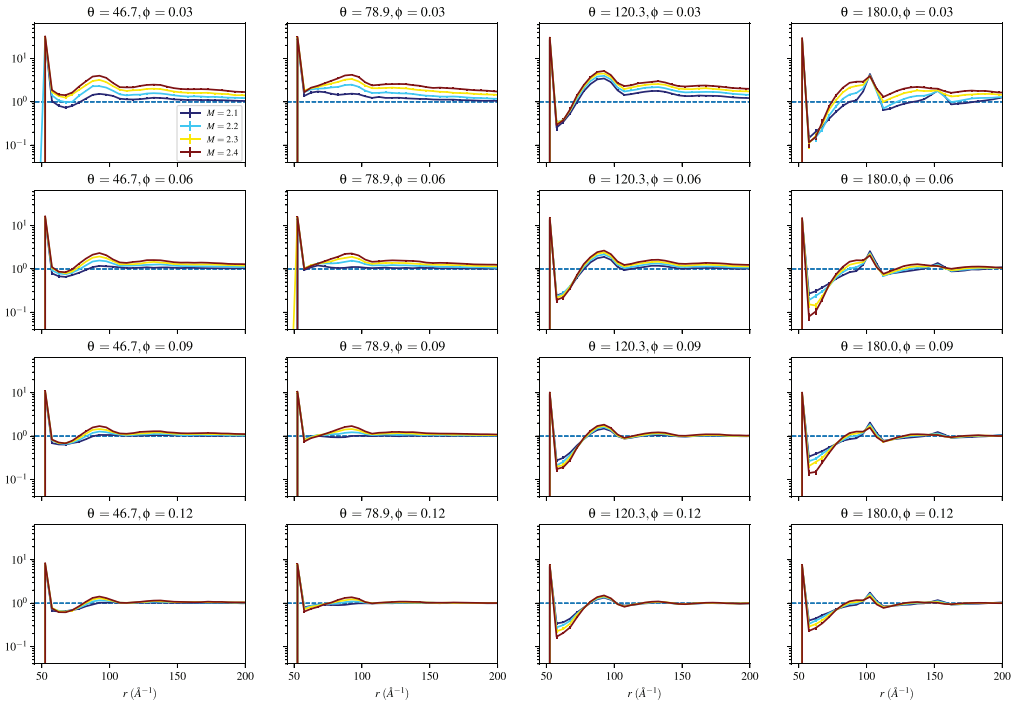

Figure S6: The effect of M on $g(r)$ for various θ and ϕ.

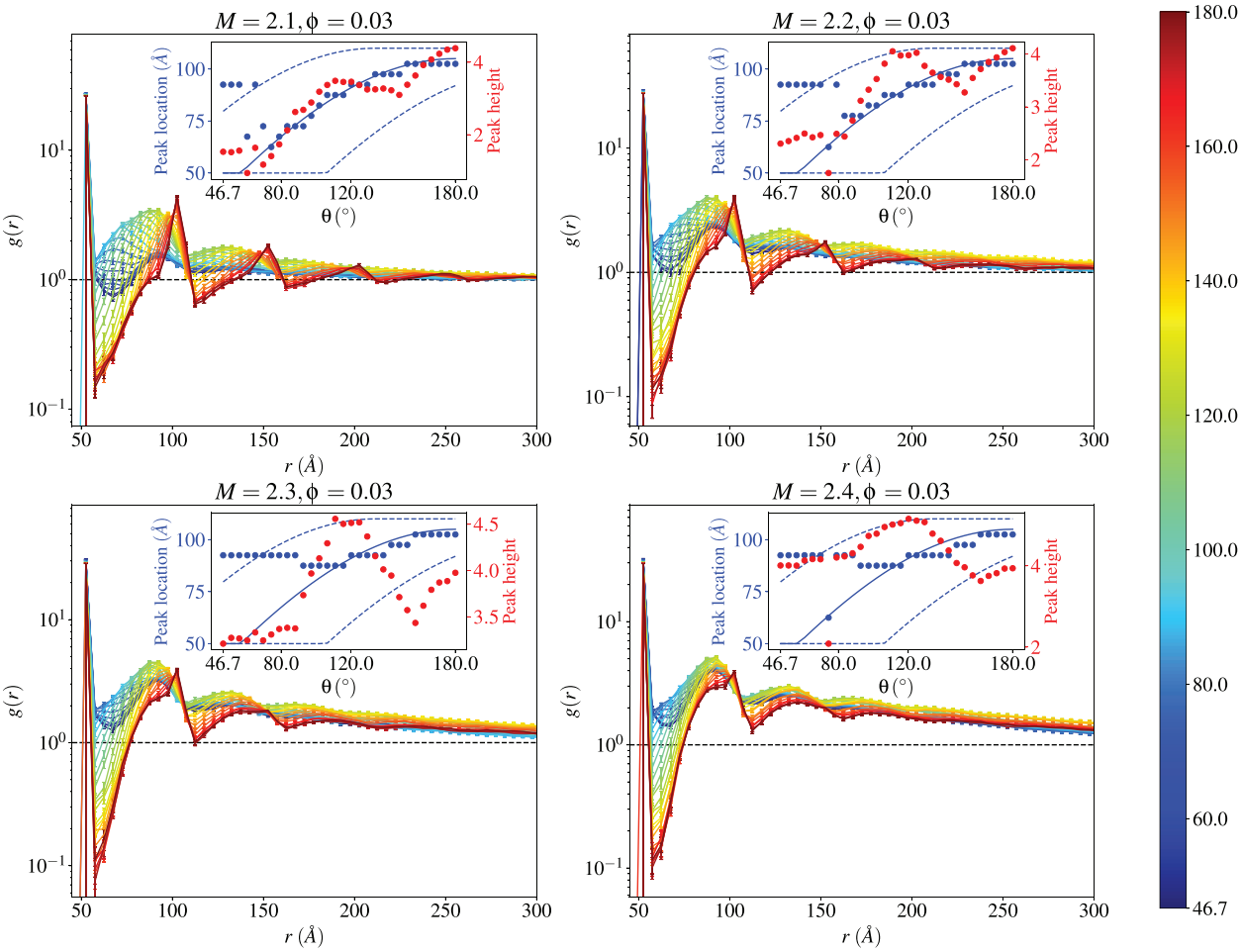

Figure S7: Radial distribution functions for $\phi = 0.03$ for all θ and M. The geometric prediction for the location of the second peak in $g(r)$ breaks down for $M > 2.2$ (insets).

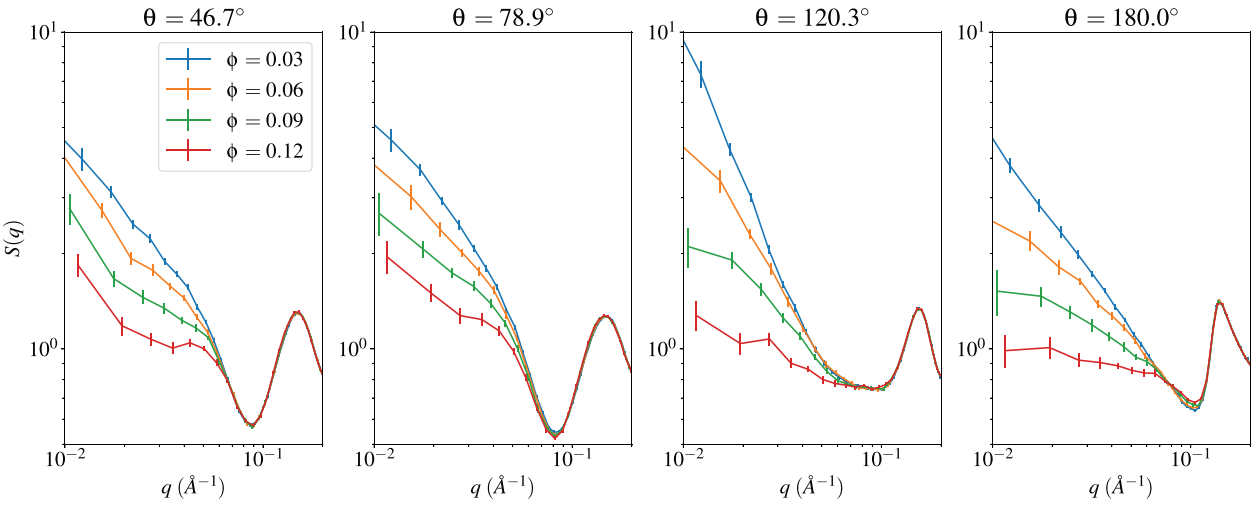

Figure S8: The change in structure factors for $M = 2.1$ with respect to ϕ, for various θ values.